Blockade of Epidermal Growth Factor Receptor Signaling in Tumor Cells and Tumor-associated Endothelial Cells for Therapy of Androgen-independent Human Prostate Cancer Growing in the Bone of Nude Mice[1]

Sun-Jin Kim,[2] Hisanori Uehara,[2] Takashi Karashima, David L. Shepherd, Jerald J. Killion, and Isaiah J. Fidler[3]

Department of Cancer Biology, The University of Texas M. D. Anderson Cancer Center, Houston, Texas 77030

ABSTRACT

Purpose: **We determined whether blockade of the epidermal growth factor receptor (EGF-R) signaling pathway by oral administration of the EGF-R tyrosine kinase inhibitor (PKI 166) alone or in combination with injectable Taxol inhibits the growth of PC-3MM2 human prostate cancer cells in the bone of nude mice.**

Experimental Design: **Male nude mice implanted with PC-3MM2 cells in the tibia were treated with oral administrations of PKI 166 or PKI 166 plus injectable Taxol beginning 3 days after implantation. The incidence and size of bone tumors and destruction of bone were determined by digitalized radiography. Expression of epidermal growth factor (EGF), EGF-R, and activated EGF-R in tumor cells and tumor-associated endothelial cells was determined by immunohistochemistry.**

Results: **Oral administration of PKI 166 or PKI 166 plus injectable Taxol reduced the incidence and size of bone tumors and destruction of bone. Immunohistochemical analysis revealed that PC-3MM2 cells growing adjacent to the bone expressed high levels of EGF and activated EGF-R, whereas tumor cells in the adjacent musculature did not. Moreover, endothelial cells within the bone tumor lesions, but not in uninvolved bone or tumors in the muscle, expressed high levels of activated EGF-R. Treatment with PKI 166 and more so with PKI 166 plus Taxol significantly inhibited phosphorylation of EGF-R on tumor and endothelial cells and induced significant apoptosis and endothelial cells within tumor lesions.**

Conclusions: **These data indicate that endothelial cells exposed to EGF produced by tumor cells express activated EGF-R and that targeting EGF-R can produce significant therapeutic effects against prostate cancer bone metastasis.**

INTRODUCTION

The major cause of death from prostate cancer is metastases that are resistant to conventional therapies (1). The metastases are often located in lymph nodes or bone (1, 2), and the specific organ microenvironment can influence the biological behavior of metastatic cells, including their response to systemic therapy (3). The outcome of organ-specific metastasis depends on multiple interactions between unique subpopulations of prostate cancer cells and specific homeostatic factors in the organ microenvironment (3, 4). More than a century ago, Stephen Paget researched the mechanisms that regulate organ-specific metastasis (*i.e.*, pattern of metastasis by different cancers). His research documented a nonrandom pattern of visceral (and bone) metastasis. This finding suggested to Paget that the process was not because of chance but because certain tumor cells (the seed) had a specific affinity for the milieu of certain organs (the soil). Metastases only resulted when the seed and soil were compatible (5). A prime example of this principle is the contribution of angiogenesis to the growth of neoplasms.

The growth and spread of prostate cancer are dependent on the formation of adequate vasculature, *i.e.*, angiogenesis (4, 6, 7). Angiogenesis consists of multiple, sequential, and interdependent steps. The onset of angiogenesis involves a change in the local equilibrium between positive and negative regulatory molecules. The major proangiogenic factors include bFGF,[4] VEGF/vascular permeability factor, IL-8, EGF, and platelet-derived growth factor (7–12).

PTKs play a key role in the control of cell proliferation (13, 14). A significant number of oncogenes and proto-oncogenes, including EGF-R, are PTKs (13–16). Under physiological conditions, the binding of EGF to its receptor, EGF-R, leads to receptor tyrosine kinase activity and subsequently to a complex cascade of events culminating in cell proliferation, which is enhanced by

Received 10/3/02; revised 12/20/02; accepted 12/20/02.
The costs of publication of this article were defrayed in part by the payment of page charges. This article must therefore be hereby marked *advertisement* in accordance with 18 U.S.C. Section 1734 solely to indicate this fact.
[1] Supported in part by Cancer Center Support Core Grant CA16672, Specialized Programs of Research Excellence (SPORE) in Prostate Cancer Grant CA90270, and SPORE in Ovarian Cancer Grant CA93639 from the National Cancer Institute, NIH.
[2] Both authors contributed equally to this work.
[3] To whom requests for reprints should be addressed, at Department of Cancer Biology-173, The University of Texas M. D. Anderson Cancer Center, 1515 Holcombe Boulevard, Houston, TX 77030. Phone: (713) 792-8577; Fax: (713) 792-8747; E-mail: ifidler@mdanderson.org.

[4] The abbreviations used are: bFGF, basic fibroblast growth factor; EGF, epidermal growth factor; EGF-R, epidermal growth factor receptor; IL, interleukin; PCNA, proliferating cell nuclear antigen; TGF, transforming growth factor; TUNEL, terminal deoxynucleotidyl transferase-mediated dUTP-biotin nick end-labeling; VEGF, vascular endothelial growth factor; PTK, protein tyrosine kinase; MAb, monoclonal antibody; IHC, immunohistochemical.

antiapoptotic effects also under the control of EGF (16). PKI 166, a novel EGF-R tyrosine kinase inhibitor of the pyrrolo-pyrimidine class (17), inhibits the intracellular domain of the EGF-R kinase, resulting in inhibition of cell proliferation and stimulation of apoptotic events (18, 19). Because increased expression of EGF, TGF-α, and EGF-R in surgical specimens of human prostate cancers correlates with rapidly progressive disease (20–24), we determined whether administration of PKI 166 to nude mice that had orthotopically implanted human prostate cancer cells in the bone marrow would block the EGF-R signaling pathway and, hence, inhibit progressive growth of experimental bone metastasis.

MATERIALS AND METHODS

PC-3MM2 Metastatic Variant of Human Prostate Cancer Cell Line. The PC-3 human prostate cancer cell line was originally obtained from the American Type Culture Collection (Rockville, MD). The PC-3M cell line was derived from a liver metastasis produced by parental PC-3 cells growing in the spleen of a nude mouse. PC-3M cells were implanted orthotopically into the prostate of nude mice, and after several cycles of *in vivo* selection, the highly metastatic PC-3MM2 line was isolated (25). The PC-3MM2 line was maintained as monolayer cultures in DMEM (Life Technologies, Inc., Grand Island, NY) supplemented with 10% fetal bovine serum, sodium pyruvate, nonessential amino acids, L-glutamine, a 2-fold vitamin solution (Life Technologies, Inc.), and penicillin-streptomycin (Flow Laboratories, Rockville, MD). Cell cultures were maintained and incubated in 5% CO_2/95% air at 37°C. Cultures were free of *Mycoplasma* and the following murine viruses: reovirus type 3; pneumonia virus; K virus; Theiler's encephalitis virus; Sendai virus; min virus; mouse adenovirus; mouse hepatitis virus; lymphocytic choriomeningitis virus; ectromelia virus; and lactate dehydrogenase virus (assayed by M. A. Bioproducts, Walkersville, MD).

Animals. Male athymic nude mice (NCI-nu) were purchased from the Animal Production Area of the National Cancer Institute-Frederick Cancer Research Facility (Frederick, MD). The mice were housed and maintained in specific pathogen-free conditions. The facilities were approved by the American Association for Accreditation of Laboratory Animal Care and met all current regulations and standards of the United States Department of Agriculture, United States Department of Health and Human Services, and the NIH. The mice were used in accordance with institutional guidelines when they were 8–12 weeks old.

Intratibial Injection of Tumor Cells. To produce bone tumors, PC-3MM2 cells were harvested from subconfluent cultures by a brief exposure to 0.25% trypsin and 0.02% EDTA. Trypsinization was stopped with medium containing 10% fetal bovine serum, and the cells were washed once in serum-free medium and resuspended in Ca^{2+}- and Mg^{2+}-free HBSS (HBSS). Cell viability was determined by trypan blue exclusion, and only single-cell suspensions of >95% viability were used to produce tumors in the tibia of mice.

Nude mice were anesthetized with Nembutal (Abbott Laboratories, North Chicago, IL). A percutaneous intraosseal injection was made by drilling a 27-gauge needle into the tibia immediately proximal to the tuberositas tibia. After penetration of the cortical bone, the needle was inserted into the shaft of the tibia, and 20 μl of the cell suspension (2×10^5 cells) were deposited in the bone cortex using a calibrated, push-button-controlled dispensing device (Hamilton Syringe Co., Reno, NV). To prevent leakage of cells into the surrounding muscles, a cotton swab was held for 1 min over the site of injection. The animals tolerated the surgical procedure well, and no anesthesia-related deaths occurred.

Therapy of Human Prostate Cancer Cells Growing in the Tibia of Athymic Nude Mice. PKI 166 (4-[*R*]-phenethylamino-6-[hydroxyl]phenyl-7*H*-pyrrolo[2,3-D]-pyrimidine), a novel EGF-R tyrosine kinase inhibitor, was synthesized and provided by Novartis Pharma (Basel, Switzerland). For *in vivo* administration, PKI 166 was dissolved in DMSO/0.5% Tween 80 and then diluted 1:20 in water (18, 19). Paclitaxel (Taxol), purchased from Bristol-Myers Squibb (Princeton, NJ) and dissolved in water for i.p. injection once per week at 200 μg/mouse.

Three days after the implantation of tumor cells in the tibia, five nude mice were killed, and the presence of actively growing cancer cells was determined by histological examination. The mice were randomized into four groups ($n = 10$) as follows: (*a*) three times per week oral administrations of vehicle solution (DMSO containing 0.5% Tween 80 diluted 1:20 in water) and once per week i.p. injection of saline; (*b*) once per week i.p. injection of 200 μg of Taxol; (*c*) three times per week oral administrations of 100 mg/kg PKI 166; and (*d*) three times per week oral administration of 100 mg/kg PKI 166 and once per week i.p. injection of 200 μg of Taxol. The mice were treated for 6 weeks. Tumor size and status of the injected bone (lysis) were evaluated by gross observation and digital radiography as described below.

Digitalized Radiography and Harvest of Tumors. After 3, 4, or 5 weeks of treatment, mice selected randomly from the different treatment groups were anesthetized with Nembutal and placed in a prone position. Digital radiography was carried out using the Faxitron (Faxitron X-Ray Corp., Wheeling, IL). Tumor incidence and size were recorded. The mice were euthanized on week 7 of the study (6 weeks of treatment) and weighed. The leg with tumor and the tumor-free contralateral leg were resected at the head of the femur and weighed. The net tumor weight was calculated by subtracting the weight of the uninjected leg from that of the leg with tumor. The presence of metastatic disease in macroscopically enlarged lymph nodes was confirmed by histological examination.

Reagents for Immunohistochemistry and TUNEL Assay. All antibodies for immunohistochemistry were purchased as follows: (*a*) rabbit anti-VEGF/vascular permeability factor, rabbit anti-fibroblast growth factor-2 (bFGF), rabbit anti-EGF, and rabbit anti-EGF-R were purchased from Santa Cruz Biotechnology (Santa Cruz, CA); (*b*) rabbit anti-phospho-EGF-R (activated EGF-R; Tyr845) was purchased from Cell Signaling Technology, Inc. (Beverly, MA); (*c*) rabbit anti-IL-8 was purchased from Biosource International (Camarillo, CA); (*d*) rat antimouse CD31-PECAM-1 was purchased from PharMingen (San Diego, CA); (*e*) mouse anti-PCNA clone PC-10 was purchased from DAKO A/S (Copenhagen, Denmark); (*f*) peroxidase-conjugated goat antirabbit IgG, peroxidase-conjugated goat antirat IgG, Texas Red-conjugated goat antirat IgG, and FITC-conjugated goat antirabbit IgG were purchased from Jackson Research Laboratories (West Grove, CA); (*g*) peroxidase-conjugated rat antimouse IgG2a was purchased from Serotec (Harlan Bioproducts for Science, Inc., Indianapolis, IN); and (*h*) Alexa Fluor 594-conjugated goat antirabbit IgG was purchased

from Molecular Probes (Eugene, OR). Stable 3,3′-diaminobenzidine (Research Genetics, Huntsville, AL) and Gill's hematoxylin (Sigma, St. Louis, MO) were used for visualization of IHC reaction and counterstaining, respectively. TUNEL was performed using a commercial apoptosis detection kit (Promega Corp., Madison, WI) with modification (18, 19).

Western Blot Analysis of EGF-R Autophosphorylation after Treatment of PC-3MM2 Cells with PKI 166. Serum-starved PC-3MM2 cells were treated for 60 min with PKI (0, 0.2, 0.4, 0.8, 1.6, and 3.2 μM), incubated with or without 40 ng/ml recombinant human EGF for 15 min, washed, scraped into PBS containing 5 mM EDTA and 1 mM sodium orthovanadate, and centrifuged; the pellet was resuspended in lysis buffer [20 mM Tris-HCl (pH 8.0), 137 mM NaCl, 10% glycerol, 2 mM EDTA, 1 mM phenylmethylsulfonyl fluoride, 20 μM leupeptin, and 0.15 unit/ml aprotinin] and centrifuged to recover insoluble protein. Immunoprecipitation was performed using MAb anti-EGF-R (clone EGF-RI) as described previously (18, 19). Immunoprecipitates were analyzed on 7.5% SDS-PAGE and transferred onto 0.45-μm nitrocellulose membranes. The filters were blocked with 3% BSA in TDS [20 mM Tris-HCl (pH 7.5) and 150 mM NaCl], probed with either polyclonal sheep antihuman EGF-R (1:1000) or monoclonal anti-phosphotyrosine (MAb 4G10; 1:2000) in TTBS (0.1% Tween 20 in TBS), and incubated with horseradish peroxidase-conjugated donkey antisheep IgG (1:2000; Sigma) or sheep antimouse IgG (1:2000), respectively, in TTBS. Protein bands were visualized by the enhanced chemiluminescence detection system.

Preparation of Tissues. Tumor tissues were cut into 2–3-mm^3 pieces that included the tibia and surrounding muscles. The fragments were fixed in 10% buffered formalin for 24 h at room temperature, washed with PBS for 30 min, decalcified with 10% EDTA (pH 7.4) or 7–10 days at 4°C, and then embedded in paraffin. The method described by Mori *et al.* (26) was used for the preparation of frozen sections with the following modifications: tumors cut into 2–3-mm^3 pieces were fixed in PLP solution (4% paraformaldehyde containing 0.075 M lysine and 0.01 M sodium periodate) for 24 h, washed with PBS for 30 min, decalcified with 10% EDTA (pH 7.4) for 7–10 days, and washed three times (once with PBS containing 10% sucrose for 4 h, once with PBS containing 15% sucrose for 4 h, and once with PBS containing 20% sucrose for 16 h). All procedures were carried out at 4°C. The tissues were then embedded in OCT compound (Miles, Inc., Elkhart, IN), frozen rapidly in liquid nitrogen, and stored at −70°C.

IHC Determination of EGF, EGF-R, Activated EGF-R, VEGF, bFGF, IL-8, PCNA, and CD31/PECAM-1. Paraffin-embedded tissues were used for identification of EGF, EGF-R, activated EGF-R, VEGF, bFGF, IL-8, and PCNA. Sections (4–6-μm thick) were mounted on positively charged Superfrost slides (Fisher Scientific, Co., Houston, TX) and dried overnight. Sections were deparaffinized in xylene, dehydrated with a graded series of alcohol [100%, 95%, and 80% ethanol/double-distilled H_2O (v/v)], and then rehydrated in PBS (pH 7.5). Sections analyzed for PCNA were microwaved for 5 min to improve "antigen retrieval." All other paraffin-embedded tissues were treated with pepsin (Biomeda, Foster City, CA) for 15 min at 37°C and washed with PBS (18). Periodate-lysine-paraformaldehyde-fixed frozen tissues used for identification of CD31/PECAM-1 were sectioned (8–10 μm), mounted on positively charged Plus slides (Fisher Scientific), and air dried for 30 min. Frozen sections were fixed in cold acetone (5 min), 1:1 acetone/chloroform (v/v; 5 min), and acetone (5 min) and washed with PBS. IHC procedures were performed as described previously (18, 19). A positive reaction was visualized by incubating the slides with stable 3,3′-diaminobenzidine for 10–20 min. The sections were rinsed with distilled water, counterstained with Gill's hematoxylin for 1 min, and mounted with Universal Mount (Research Genetics). Control samples exposed to secondary antibody alone showed no specific staining. Dilutions of primary antibodies were as follows: (*a*) EGF, 1:100; (*b*) EGF-R, 1:50; (*c*) phosphorylated EGF-R, 1:50; (*d*) VEGF, 1:100; (*e*) bFGF, 1:100; (*f*) IL-8, 1:25; (*g*) PCNA, 1:100; and (*h*) CD31/PECAM-1, 1:400. Peroxidase-conjugated secondary antibodies were used for immunohistochemistry of EGF, EGF-R, VEGF, bFGF, IL-8, and PCNA.

Alexa Fluor 594-conjugated secondary antibody at 1:400 dilution was used for immunohistochemistry of phosphorylated EGF-R. The sections were rinsed with distilled water and mounted with Vectashield (mounting medium with 4′,6-diamidino-2-phenylindole; Vector Laboratories, Inc., Burlingame, CA), which gave nuclear staining of blue fluorescence.

Immunofluorescence Double Staining for CD31/PECAM-1 (Endothelial Cells) and EGF-R or TUNEL (Apoptotic Cells). PLP-fixed frozen tissues were sectioned (8–10 μm), mounted on positively charged slides, air dried for 30 min, and fixed in cold acetone for 5 min, in 1:1 acetone/chloroform (v/v) for 5 min, and in acetone for 5 min. The samples were washed three times with PBS, incubated with protein-blocking solution containing 5% normal horse serum and 1% normal goat serum in PBS for 20 min at room temperature, and then incubated with a 1:400 dilution of rat monoclonal antimouse CD31 antibody (human cross-reactive) for 18 h at 4°C. After the samples were rinsed four times with PBS for 3 min each, the slides were incubated with a 1:200 dilution of secondary goat antirat antibody conjugated to Texas Red for 1 h at room temperature in the dark. Samples were then washed twice with PBS containing 0.1% Brij and once with PBS for 5 min.

EGF-R immunostaining was performed after CD31 staining. Samples were incubated with protein-blocking solution for 5 min at room temperature and incubated with a 1:50 dilution of rabbit polyclonal antihuman EGF-R antibody (mouse cross-reactive) for 18 h at 4°C. The samples were then rinsed four times with PBS for 3 min each. The slides were incubated with a 1:200 dilution of secondary goat antirabbit antibody conjugated to FITC for 1 h at room temperature. Samples were washed twice with PBS containing 0.1% Brij and once with PBS for 5 min and mounted with Vectashield.

TUNEL was performed using an apoptosis detection kit with the following modifications: samples were fixed with 4% paraformaldehyde (methanol free) for 10 min at room temperature; washed twice with PBS for 5 min; and then incubated with 0.2% Triton X-100 for 15 min at room temperature. After being washed twice with PBS for 5 min, the samples were incubated with equilibration buffer (from kit) for 10 min at room temperature. The equilibration buffer was drained, and reaction buffer containing equilibration buffer, nucleotide mix, and terminal deoxynucleotidyl transferase enzyme was added to the

tissue sections. The sections were incubated in a humid atmosphere at 37°C for 1 h in the dark. The reaction was terminated by immersing the samples in 2× SSC for 15 min. Samples were washed three times for 5 min to remove unincorporated fluorescein-dUTP. For quantification of endothelial cells, the samples were incubated with 300 μg/ml Hoechst stain for 10 min at room temperature. Fluorescence bleaching was minimized by treating slides with an enhancing reagent (Prolong solution). Immunofluorescence microscopy was performed using a ×40 objective on an epifluorescence microscope equipped with narrow band pass excitation filters mounted on a filter wheel (Ludl Electronic Products, Hawthorne, NY) to individually select for green, red, and blue fluorescence. Images were captured using a Sony 3-chip camera (Sony Corporation of America, Montvale, NJ) mounted on a Zeiss universal microscope (Carl Zeiss, Thornwood, NY) and Optimas Image Analysis software (Bioscan, Edmond, WA) installed on a Compaq computer with Pentium chip, a frame grabber, an optical disk storage system, and a Sony Mavigraph UP-D7000 digital color printer (Tokyo, Japan). To produce prints, images were further processed using Adobe PhotoShop software (Adobe Systems, Mountain View, CA) to make figures. Endothelial cells were identified by red fluorescence, and DNA fragmentation was detected by localized green and yellow fluorescence within the nucleus of apoptotic cells. Quantification of apoptotic endothelial cells was expressed as an average of the ratio of apoptotic endothelial cells to the total number of endothelial cells in 5–10 random 0.011-mm^2 fields at ×400 magnification. For the quantification of total TUNEL expression, the number of apoptotic events was counted in 10 random 0.159-mm^2 fields adjacent to bone and in muscles at ×100 magnification.

Quantification of Mean Vessel Density and PCNA. For the quantification of microvessel density, 10 random 0.159-mm^2 fields adjacent to the bone and 10 fields of tumor in the muscles at ×100 magnification were captured for each tumor, and mean vessels were quantified according to the method described previously (18, 19, 27).

Statistical Analysis. Tumor incidence (χ^2 test) and weight (Mann-Whitney *t* test), incidence of lymph node metastasis (χ^2 test), and expression of CD31/PECAM-1, CD31/TUNEL, TUNEL, and PCNA (unpaired Student's *t* test) were compared.

RESULTS

Inhibition of EGF-R Autophosphorylation in Human Prostate Cancer Cells by PKI 166. In the first set of experiments, we determined whether *in vitro* treatment of PC-3MM2 cells with PKI 166 could inhibit EGF-stimulated tyrosine phosphorylation of the EGF-R. PC-3MM2 cells incubated for 15 min in medium free of serum but containing EGF exhibited high levels of autophosphorylated EGF-R (M_r 170,000 band) as detected by anti-phosphotyrosine antisera on Western blots of anti-EGF-R-immunoprecipitated cell lysates (Fig. 1). Pretreatment of cells with PKI 166 for 1 h followed by a 15-min treatment with EGF inhibited the autophosphorylation in a dose-dependent manner (0–3.2 μM). The identity of the M_r 170,000 band was confirmed by Western blot using anti-EGF-R antisera.

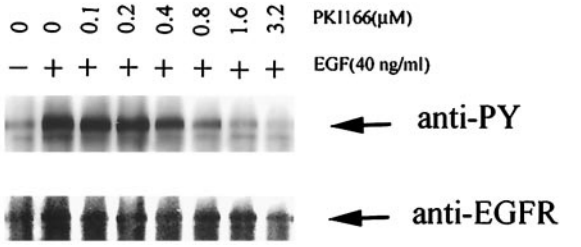

Fig. 1 Inhibition of EGF-induced autophosphorylation of EGF-R. Serum-starved PC-3MM2 human prostate cancer cells were treated in culture for 1 h with PKI 166 (0, 1.6, and 3.2 μM) and then incubated for 15 min with or without 40 ng/ml recombinant human EGF. The cells were washed and lysed. Insoluble proteins were immunoprecipitated with an anti-EGF-R MAb, separated by 7.5% SDS-PAGE, transferred to nitrocellulose, and sequentially probed with antisera to phosphotyrosine (*anti-pY*) and EGF-R. The immunoreactive proteins were detected by incubating the blot with the corresponding peroxidase-conjugated IgG and visualized using the enhanced chemiluminescence system. Pretreatment of the cells with PKI 166 for 1 h, followed by a 15-min treatment with EGF, inhibited the autophosphorylation in a dose-dependent manner.

Taxol, at a concentration of 10 μM, did not affect the autophosphorylation of EGF-R (data not shown).

Inhibition of Prostate Cancer Cell Growth and Metastasis. Three days after the implantation of PC-3MM2 tumor cells into the tibia of athymic nude mice, five mice were killed, and the presence of tumor cells was confirmed by histology. The remaining mice were than randomized into four treatment groups of 10 mice each. The first group received three weekly oral administrations of PKI 166 (100 mg/kg/dose). The second group was injected i.p. once per week with 200 μg of Taxol, a third group received three oral doses of PKI 166 (100 mg/kg) per week and one dose of Taxol per week i.p. (200 μg/dose), and the last group received three oral doses per week of vehicle solution for PKI 166 (DMSO/water) and one i.p. injection of water per week. All mice were killed on day 35 (5 weeks of treatment) because the control mice had large tumors in the injected leg. The data of two independent experiments were very similar and therefore are combined in Table 1. All control mice had large tumors in the tibia and surrounding muscles (median weight, 2.7 g), and all mice had lymph node metastasis. Treatment with Taxol (200 μg/dose once per week) did not decrease the incidence or size of the tumors in the bone or the incidence of lymph node metastasis. Three doses of PKI 166 (100 mg/kg) significantly decreased tumor size (median weight, 1.5 g) and the incidence of lymph node metastasis (55%) as compared with control mice. The combination of oral PKI 166 and i.p. Taxol produced highly significant reductions in PC-3MM2 bone lesions. Specifically, the tumor incidence was reduced from 20 of 20 in control mice to 11 of 20 in the treated mice ($P < 0.01$). The median size of the tumors in the tibia and surrounding muscles was significantly reduced to 0.4 g ($P < 0.001$), and the incidence of lymph node metastasis was significantly reduced to 35% ($P < 0.001$).

Digital radiography of representative hind legs of mice from the four treatment groups are shown in Fig. 2. Severe lysis of the tibia was found in control mice and mice treated with Taxol. In mice given oral PKI 166, bone integrity was improved.

Table 1 Therapy of human prostate carcinoma growing in the bone of nude mice

	Bone lesion		
Treatment group[a]	Incidence[b]	Tumor weight (g) (mean ± SD)	Lymph node metastasis (%)
Control	20/20	2.8 ± 1/1	100
Taxol	18/20	2.1 ± 1.5	90
PKI 166	15/20[c]	1.5 ± 1.4[c]	55[d]
PKI 166 + Taxol	11/20[d]	0.8 ± 0.7[d]	35[d]

[a] Human prostate cancer cells were injected into the tibia of nude mice. Three days later, groups of mice were treated with oral feeding of PKI 166 (100 mg/kg, thrice weekly) alone, weekly i.p. injection of Taxol (200 μg) alone, PKI 166 and Taxol, or water (control).
[b] Number of positive mice/number of mice receiving injections.
[c] $P < 0.05$.
[d] $P < 0.001$ *versus* control.

The combination of PKI 166 plus Taxol was most successful in preserving the bone structure and preventing bone lysis (Fig. 2).

Histology and IHC Analyses. The PC-3MM2-induced lytic lesions in the bone expanded into and grew in the surrounding muscles. Tumor specimens from the bone and muscles were processed for routine histology and IHC analyses. Tumors treated with PKI 166 and Taxol had some necrotic zones. Immunohistochemistry using specific anti-EGF, EGF-R, activated EGF-R, bFGF, VEGF, and IL-8 antibodies demonstrated striking differences in the level of expression (Fig. 3). The tumor cells growing adjacent to bone tissue expressed high levels of EGF, EGF-R, and activated EGF-R, whereas tumor cells growing in the muscle did not. The expression of bFGF, VEGF, and IL-8 also differed between tumor cells growing adjacent to bone (high expression) and those growing in the muscle (low expression; Fig. 3). Immunohistochemistry of bone and muscle lesions from control mice and mice treated with Taxol, PKI 166, or PKI 166 and Taxol did not demonstrate differences in expression of EGF, EGF-R, bFGF, VEGF, and IL-8. These data were expected because PKI 166 inhibits only phosphorylation of the EGF-R, not its expression (18, 19) or the expression of the other cytokines studied here.

The most striking results deal with the activation status of EGF-R in tumors adjacent to the bone or in the muscle of mice treated with PKI 166 alone or with PKI 166 and Taxol (Fig. 4). In all mice, only the tumor cells growing adjacent to bone tissue expressed EGF-R as detected by specific anti-EGF-R antibodies. Immunostaining with antibodies specific against tyrosine-phosphorylated (activated) EGF-R demonstrated that in control mice or mice treated with Taxol, tumor cells adjacent to bone (but not in the muscles) expressed phosphorylated EGF-R. In contrast, tumor cells adjacent to the bones of mice treated with PKI 166 or PKI 166 plus Taxol did not express activated EGF-R (Fig. 4), confirming that PKI 166 inhibits the phosphorylation of EGF-R under both *in vitro* and *in vivo* conditions.

The decrease in tumor size in mice treated with PKI 166 or with PKI 166 and Taxol could have been due to inhibition of tumor cell division, increased tumor cell apoptosis, or both. In the next set of IHC analyses, we determined the number of $PCNA^+$ and $TUNEL^+$ cells in PC-3MM2 tumors harvested from control and treated mice (Table 2). No significant differences in the number of $PCNA^+$ cells were found between tumor lesions adjacent to the bone (136 ± 29) and those in the muscle (130 ± 22). Taxol treatment decreased the number of $PCNA^+$ cells in both tumors adjacent to the bone and tumors growing in the muscle to 78 ± 33 and 75 ± 29, respectively ($P < 0.001$). In contrast, PKI 166 treatment decreased the number of $PCNA^+$ cells in tumors growing adjacent to the bone (88 ± 20; $P < 0.001$) but did not decrease the number of $PCNA^+$ cells in tumors growing in the muscle (122 ± 20). The decrease in $PCNA^+$ cells in tumors of mice treated with Taxol plus PKI 166 differed between tumors growing adjacent to the bone (39 ± 16) and those growing in the muscle (72 ± 25).

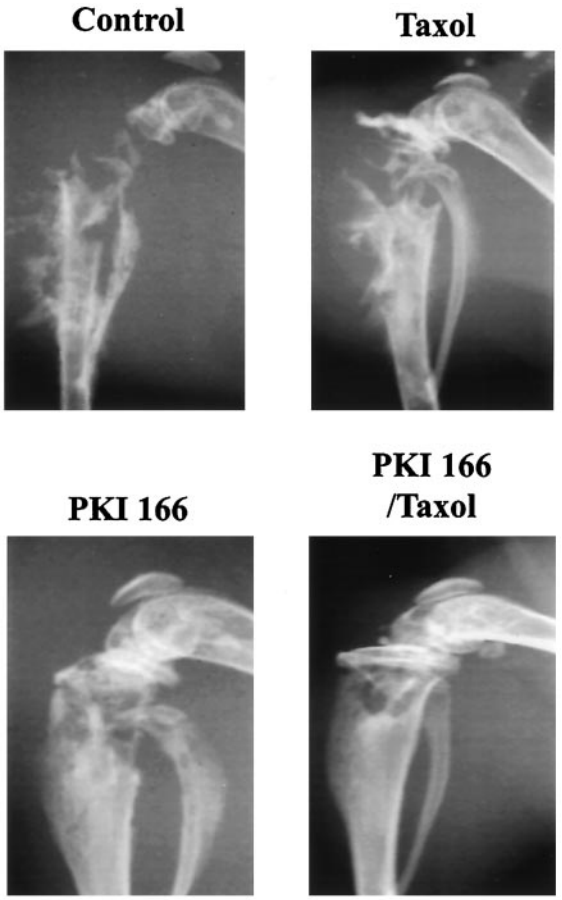

Fig. 2 Digitalized radiography of PC-3MM2 tumors in hind legs of nude mice. Nude mice received injection into the tibia of human PC-3MM2 prostate cancer cells. After 5 weeks of treatment with PKI 166, Taxol, or PKI 166 and Taxol, the mice were anesthetized with Nembutal and placed in a supine position for digital radiography. The PC-3MM2 cells produced lysis of the tibia in control mice and in mice treated with Taxol. In contrast, treatment with PKI 166 alone, and more so with PKI 166 plus Taxol, significantly prevented lysis of the bone.

Treatment with Taxol or PKI 166 produced a significant increase in apoptosis ($TUNEL^+$ cells) in the PC-3MM2 cells growing adjacent to the bone (Table 2). Specifically, the number of $TUNEL^+$ cells in control, Taxol-treated, and PKI 166-treated mice was 8 ± 2, 32 ± 15, and 29 ± 14, respectively ($P < 0.001$). Treatment with PKI 166 and Taxol produced a highly

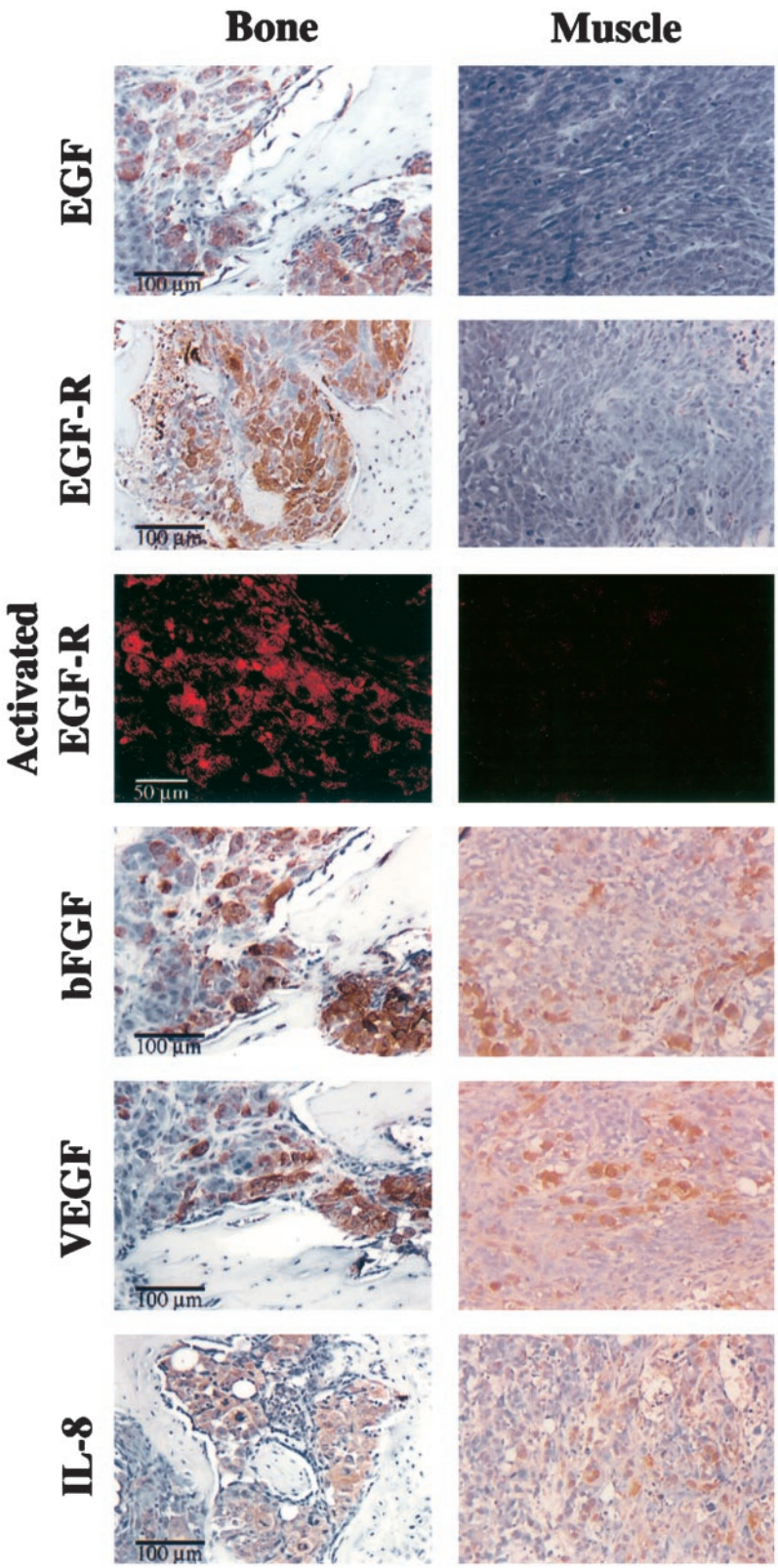

Fig. 3 Differential expression of EGF, EGF-R, activated EGF-R, bFGF, VEGF, and IL-8 by PC-3MM2 cells growing in the bone or surrounding muscles. IHC analysis of tumor tissues demonstrates that tumor cells growing adjacent to bone tissue express high levels of EGF, EGF-R, and activated EGF-R, whereas tumor cells growing in the muscles do not. The expression of bFGF, IL-8, and VEGF also differed between tumor cells growing in the bone (high intensity) and those in the muscles (low intensity).

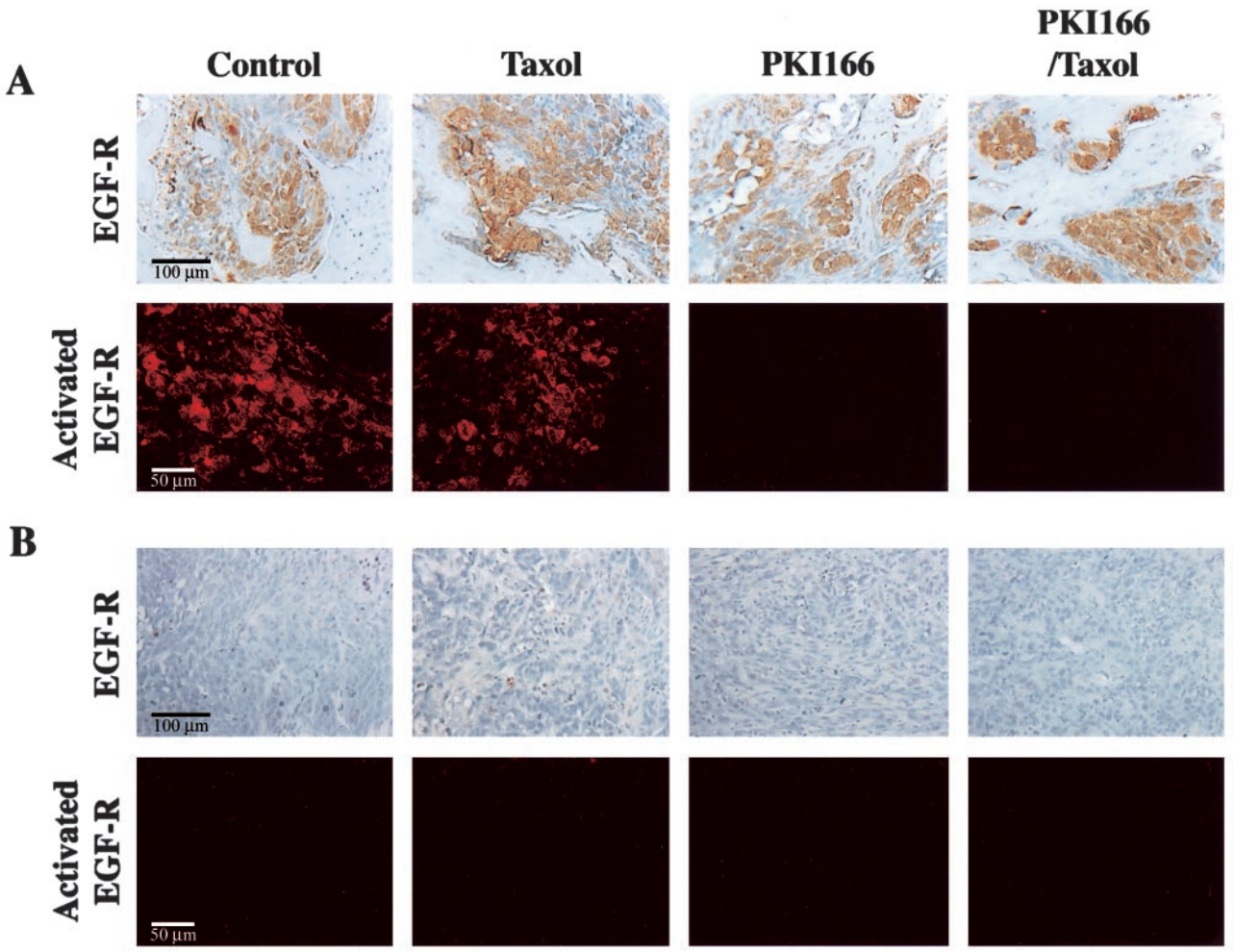

Fig. 4 IHC determination of EGF-R and activated EGF-R in human prostate cancer cells growing in the bone (*A*) and surrounding muscles (*B*) of nude mice. Human prostate cancer lesions from the bone of nude mice were harvested and processed for histology and IHC analyses after 5 weeks of treatment. Tissue sections were stained for expression of tyrosine-phosphorylated activated EGF-R (Alexa Fluor 594, *red fluorescence*) and total EGF-R. In all treatment groups, tumor cells adjacent to bone tissue stained positive for EGF-R. In contrast, tumor cells growing in the muscle did not express EGF-R. Tumor cells adjacent to bone tissue of control mice or mice treated with Taxol alone stained positive for activated EGF-R. Treatment with PKI 166 or PKI 166 plus Taxol inhibited phosphorylation (activation) of the EGF-R in the bone lesion of human prostate cancer.

significant induction of apoptosis (71 ± 20 $TUNEL^+$ cells; $P < 0.001$). However, in the PC-3MM2 tumors growing in the muscle, only treatment with Taxol or Taxol plus PKI 166 induced significant levels of apoptosis (29 ± 14 $TUNEL^+$ cells; $P < 0.001$). The combination of PKI 166 and Taxol did not produce additive apoptosis in tumor cells growing in the muscle (34 ± 17 $TUNEL^+$ cells).

Mean Vessel Density. In the next set of IHC studies, we determined the mean vessel density in the PC-3MM2 lesions (Table 2). No discernible differences in mean vessel density were found between tumor lesions adjacent to the bone (54 ± 16) and those in the muscle (52 ± 12) of control mice (Table 2). In PC-3MM2 tumors adjacent to the bone, treatment with Taxol or PKI 166 decreased the number of endothelial cells (CD31/PECAM-1^+) to 38 ± 16 and 35 ± 14, respectively. The combination therapy of PKI 166 plus Taxol produced the most significant decrease in mean vessel density to 20 ± 14 ($P < 0.001$). In the PC-3MM2 lesions growing in the muscle, treatment with Taxol or Taxol plus PKI 166 decreased mean vessel density from 52 ± 21 (control mice) to 36 ± 17 and 34 ± 19, respectively ($P < 0.01$). Treatment with PKI 166 alone did not decrease mean vessel density in the tumors.

Immunofluorescence Double Staining for CD31/PECAM-1 (Endothelial Cells) and EGF-R or TUNEL (Apoptotic Cells). In the last set of experiments, we determined whether endothelial cells can express the EGF-R and whether treatment with Taxol, PKI 166, or both can induce apoptosis of endothelial cells within the tumors. Endothelial cells within PC-3MM2 tumors in the bone (but not in the muscle) expressed EGF-R on their surface (Fig. 5). We base this conclusion on the CD31/EGF-R fluorescent double labeling technique, which revealed that endothelial cells in the bone lesions of control and treated mice stained yellow (CD31/PECAM, Texas Red; EGF-R, FITC green). For studies of apoptosis, the CD31/

Table 2 Immunohistochemical analysis of human prostate carcinoma in the bone of control and treated nude mice

	Bone				Muscle			
	Tumor cells		Endothelial cells		Tumor cells		Endothelial cells	
Treatment group[a]	PCNA^{+}[b]	TUNEL^{+}[b]	CD31^{+}[b]	% TUNEL (range)[c]	PCNA^{+}[b]	TUNEL^{+}[b]	CD31^{+}[b]	% TUNEL (range)[c]
Control	136 ± 29	8 ± 2	54 ± 16	2 (0–7)	130 ± 22	7 ± 2	52 ± 21	3 (0–6)
Taxol	78 ± 33[d]	32 ± 15[d]	38 ± 16	5 (0–16)	75 ± 29[d]	19 ± 14[d]	36 ± 16	6 (0–15)
PKI 166	88 ± 20[d]	29 ± 14[d]	35 ± 14	9 (0–15)[d]	122 ± 20	7 ± 3	50 ± 18	4 (0–8)
PKI 166 + Taxol	39 ± 16[d,e]	71 ± 20[d,e]	20 ± 14[d,e]	16 (0–23)[d,e]	72 ± 25[d]	34 ± 17[d]	34 ± 19	6 (0–17)

[a] Human prostate cancer cells were injected into the tibia of nude mice. Three days later, groups of mice were treated with oral feedings of PKI 166 (100 mg/kg, thrice weekly) alone, weekly i.p. injection of Taxol (200 μg) alone, PKI 166 and Taxol, or water (control).
[b] Mean ± SD.
[c] Median of the ratio of apoptotic endothelial cells to total number of endothelial cells in 5–10 random 0.011-mm^2 fields at ×400.
[d] $P < 0.001$ as compared with controls.
[e] $P < 0.05$ as compared with the group treated with Taxol alone.

TUNEL fluorescent double labeling technique revealed that endothelial cells within bone lesions stained yellow (CD31/PECAM, Texas Red; TUNEL, FITC green). Endothelial cells in the muscle tumors were EGF-R negative. Apoptosis of these endothelial cells was only found in mice treated with Taxol. Endothelial cells in uninvolved bones (contralateral leg) did not express EGF-R on their surface, and apoptosis of endothelial cells was not observed with treatment of PKI 166 plus Taxol.

The median percentage of apoptotic endothelial cells in bone lesions of control mice was 2% (range, 0–7%). In mice treated with PKI 166, it was 9% (range, 0–15%; $P < 0.001$). Treatment with Taxol induced a median of 5% (range, 0–16%) apoptosis. The combination therapy of PKI 166 and Taxol induced 16% (range, 0–23%) apoptosis ($P < 0.001$). In the muscle lesions, treatment with Taxol alone or with Taxol plus PKI 166 induced 6% apoptosis in endothelial cells (Table 2). No additional apoptosis of endothelial cells was found in these tumors from mice treated with PKI 166 or PKI 166 plus Taxol. These results suggest that PKI 166 can induce apoptosis only in endothelial cells that express EGF-R.

DISCUSSION

Our data show that human prostate cancer cells growing adjacent to mouse bone expressed high levels of EGF, EGF-R, and phosphorylated EGF-R. Moreover, endothelial cells within these tumor lesions also expressed activated EGF-R, whereas endothelial cells in the uninvolved bone marrow or in tumors growing in the muscles did not. Similar to the clinical experience with taxane-based regimens (28, 29), systemic administration of Taxol did not inhibit tumor growth or destruction of bone. In sharp contrast, blockade of EGF-R signaling by oral administration of the EGF-R tyrosine kinase inhibitor PKI 166 or PKI 166 combined with once per week i.p. injections of Taxol significantly inhibited the incidence and size of the bone lesions, prevented lysis of the bone as determined by radiographic and histological examination, and significantly reduced the incidence of lymph node metastasis. IHC analysis of the PC-3MM2 tumors growing in the bone demonstrated inhibition of activated EGF-R in lesions from mice treated with PKI 166 alone or with PKI 166 combined with Taxol. This effect was associated with inhibition of tumor cell proliferation (PCNA^{+} cells) and an increase in tumor cell apoptosis (TUNEL^{+} cells). The oral administration of PKI 166 alone or in combination with Taxol also produced apoptosis in tumor-associated endothelial cells (TUNEL^{+}/CD31^{+} cells), corresponding to a significant decrease in microvessel density.

The progressive growth of many human carcinomas, including prostate, colon, pancreatic, gastric, ovarian, renal, bladder, breast, and non-small cell lung cancer, has been associated with expression of EGF-R (21, 30–34). Overexpression of EGF-R and one of its ligands has been shown to correlate with rapidly progressive disease (35). Our present results closely agree with previous studies showing that targeting the EGF-R by the anti-EGF-R C225 antibody in combination with radiation or chemotherapy can significantly inhibit the growth of human tumors in nude mice (36–42). The present results also agree with our previously published data (18) showing that blockade of EGF-R signaling with PKI 166 inhibits growth of human pancreatic carcinoma in nude mice and produces apoptosis of tumor-associated endothelial cells.

Detailed histological and IHC analyses revealed that robust expression of EGF and EGF-R in PC3MM2 cells was restricted to cells growing adjacent to the mouse bone. Tumor cells growing in the musculature (subsequent to lysis of the bone) expressed low to no EGF or EGF-R (Fig. 3). Because the PC-3MM2 cells express EGF and EGF-R when growing in the prostate (data not shown), the absence of these proteins in cells growing in the muscle could be due to an inhibitory mechanism unique to the musculature. This possibility, which supports the venerable "seed and soil" hypothesis (5), is under active investigation. The robust angiogenesis in these lesions could well be due to the low but apparently sufficient expression of bFGF, IL-8, and VEGF (Fig. 3) or to other proangiogenic molecules, such as IL-1 and TNF-α (7, 8, 12). TGF-β has been shown to increase expression of EGF and EGF-R in tumor cells (43–45). Because TGF-β is produced in bone subsequent to injury (46), the expression of EGF-R in the PC3-MM2 cells can reflect their proximity to the injured bone, *i.e.*, TGF-β. Even more striking was the finding that endothelial cells in the tumor lesions expressed EGF-R and activated EGF-R, whereas endothelial cells 1–2 mm away from the lesions did not. The expression of EGF-R by tumor-associated endothelial cells could have been due to two parallel (and additive) mechanisms. First, the majority of endothelial cells in normal tissues and organs are quies-

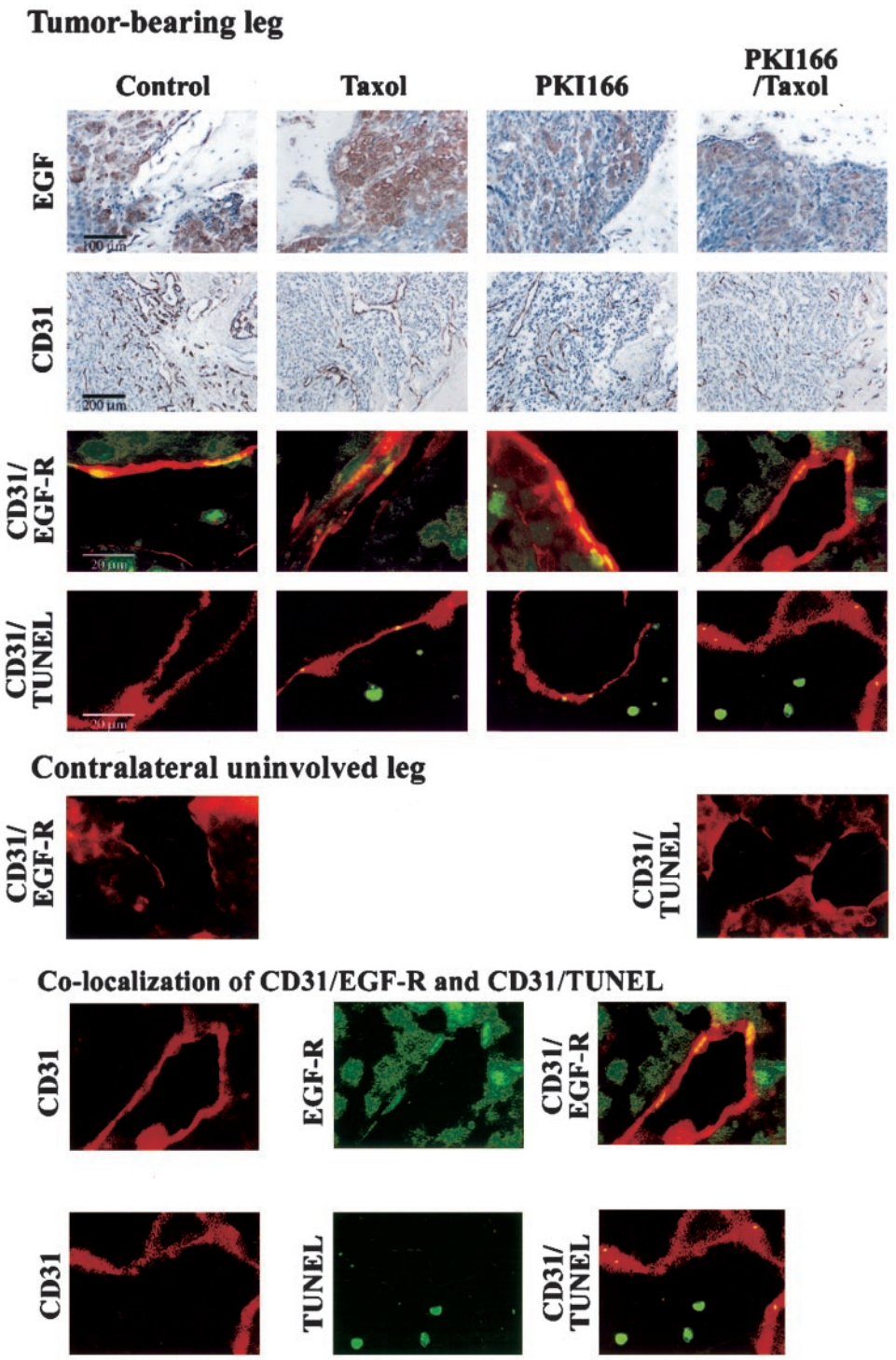

Fig. 5 Immunohistochemistry and immunofluorescent double labeling for CD31/PECAM-1 (Texas Red) and EGF-R (FITC green), or TUNEL (FITC green). Images captured for endothelial cells (CD31 *red*) are overlapped with images captured for EGF-R (*green*) or apoptosis (TUNEL *green*) and expression of two markers, CD31/EGF-R or CD31/TUNEL (both cells emitted *yellow*). Tumor lesions in the bone contained numerous blood vessels ($CD31^+$ structures), and mean vascular densities were significantly reduced in the combined treatment group. Tumor cells growing adjacent to bone tissue expressed EGF and EGF-R. Endothelial cells (*red*) within the bone lesions also expressed EGF-R (*fluorescent yellow*). Treatment of mice with PKI 166 plus Taxol induced apoptosis of tumor cells (*green*) and endothelial cells (*yellow*) within the bone lesions. Treatment of mice with PKI 166 plus Taxol did not induce apoptosis in the endothelial cells in the tumors growing in the muscles.

cent and do not divide. In contrast, many endothelial cells within progressive neoplasms are actively dividing, and dividing endothelial cells have been shown to express low levels of EGF-R (47). Mere proliferation, however, is not sufficient to account for high-level expression of EGF-R or its activation. Recent work from our laboratory revealed that murine endothelial cells do indeed express EGF-R when exposed in culture to EGF or TGF-α in a dose-dependent manner. Specifically, the expression of EGF-R and activated EGF-R required incubation of endothelial cells with >20 ng/ml EGF (47). As seen in Fig. 3, PC-3MM2 cells growing adjacent to the bone cortex produce EGF, whereas tumor cells growing at a distance from the bone do not.

The level of expression of EGF-R by endothelial cells within the bone tumor lesions could be related to the concentration of EGF in the microenvironment. The finding that the expression of growth factor receptors (and their activation) on endothelial cells is conditioned by the organ microenvironment is another example that supports the venerable "seed and soil" hypothesis (4, 5, 10). In any event, the expression of activated EGF-R in tumor-associated endothelial cells, but not in endothelial cells within the uninvolved organ, makes EGF-R an attractive target for specific antivascular therapy.

Treatment of mice with PKI 166 and Taxol significantly decreased the number of bone tumor-associated endothelial cells (but not the number of endothelial cells in muscle lesions). The increase of apoptosis in endothelial cells providing vasculature to the bone tumors could be attributed to blockade of EGF-R, which results in cellular arrest at the G_1 restriction point (34, 37, 38) and a decrease in expression of proangiogenic molecules that serve as survival factors for immature blood vessel endothelial cells (48–51). The decrease in production of proangiogenic molecules can prevent the recovery of dividing endothelial cells damaged by Taxol and hence lead to increased apoptosis in tumor-associated, dividing endothelial cells. Moreover, EGF-R and its associated PTKs are known to regulate apoptosis (52, 53), and inactivation of EGF-R PTK has been shown to inhibit EGF-induced receptor autophosphorylation, mitogen-activated protein kinase activation, phosphatidylinositol 3′-kinase activity, entry into S phase, and cyclin E-associated kinase activity, all leading to accumulation of cells in the G_1 phase of the cell cycle (54). Induction of endothelial cell apoptosis was found only in cells stimulated with EGF (or TGF-α), *i.e.*, cells that expressed the activated EGF-R. Our data agree with a previously published report that inhibition of EGF-R tyrosine kinase by another PTK inhibitor, ZD 1839 (Iressa), can produce antiangiogenic effects (55).

Cancers are biologically heterogeneous, and their phenotype is modified by the organ environment (3, 4). Successful treatment of cancers and their metastases therefore requires multiple agents. The results shown here clearly demonstrate that treatment with PKI 166 and Taxol produces a decrease in tumor size and incidence of metastasis. The combination of PKI 166 plus Taxol, however, produces additive effects demonstrable by induction of apoptosis in tumor cells and, more so, tumor-associated endothelial cells. These results confirm that a heterogeneous disease should be treated by multiple modality therapy.

The outcome of cancer metastasis is controlled by the interaction of specific tumor cells (the seed) with unique host microenvironment (the soil; Ref. 56). Organ-specific angiogenesis is essential for progressive growth of metastases. The demonstration that endothelial cells in experimental prostate cancer bone metastases express growth factor receptor differentially from endothelial cells in uninvolved zones of the same organ offers an exciting new approach to the specific therapy of a devastating disease.

ACKNOWLEDGMENTS

We thank Walter Pagel for critical editorial review and Lola López for expert assistance in the preparation of the manuscript.

REFERENCES

1. Landis, S. H., Murray, T., and Bolden Wingo, P. A. Cancer statistics 1999. Cancer (Phila.), *49:* 8–31, 1999.

2. Soh, S., Kattan, M. W., Berkman, S., Wheeler, T. M., and Scardino, P. T. Has there been a recent shift in the pathological features and prognosis of patients treated with radical prostatectomy? J. Urol., *157:* 2212–2218, 1997.

3. Fidler, I. J. Critical factors in the biology of human cancer metastasis: Twenty-eighth G. H. A. Clowes Memorial Award Lecture. Cancer Res., *50:* 6130–6138, 1990.

4. Fidler, I. J. Modulation of the organ microenvironment for the treatment of cancer metastasis. J. Natl. Cancer Inst. (Bethesda), *87:* 1588–1592, 1995.

5. Paget, S. The distribution of secondary growths in cancer of the breast. Lancet, *1:* 571–573, 1889.

6. Folkman, M. J. The role of angiogenesis in tumor growth. Semin. Cancer Biol., *3:* 65–71, 1992.

7. Auerbach, W., and Auerbach, R. Angiogenesis inhibition: a review. Pharmacol. Ther., *63:* 265–311, 1994.

8. Bouck, N., Stellmach, V., and Hsu, S. C. How tumors become angiogenic. Adv. Cancer Res., *69:* 135–174, 1996.

9. Dvorak, H. F. Tumors: wounds that do not heal. N. Engl. J. Med., *315:* 1650–1659, 1986.

10. Fidler, I. J. Angiogenic heterogeneity: regulation of neoplastic angiogenesis by the organ microenvironment. J. Natl. Cancer Inst. (Bethesda), *93:* 1040–1041, 2001.

11. Folkman, J. Clinical applications of research on angiogenesis. N. Engl. J. Med., *333:* 1753–1763, 1995.

12. Hanahan, D., and Folkman, J. Patterns and emerging mechanisms of the angiogenic switch during tumorigenesis. Cell, *86:* 353–364, 1996.

13. Ullrich, A., and Schlessinger, J. Signal transduction by receptors with tyrosine kinase activity. Cell, *61:* 203–212, 1990.

14. Yarden, Y., and Ullrich, A. Growth factor receptor tyrosine kinases. Annu. Rev. Biochem., *57:* 443–478, 1988.

15. Kaplan, D. R., Martin-Zanca, D., and Parada, L. F. Tyrosine phosphorylation and tyrosine kinase activity of the *trk* proto-oncogene product induced by NGF. Nature (Lond.), *350:* 158–160, 1991.

16. Wells, A. EGF receptor. Int. J. Biochem. Cell Biol., *31:* 637–643, 1999.

17. Traxler, P., Buchdunger, E., Furet, P., Gschwind, H-P., Ho, P., Mett, H., O'Reilly, T., Pfaar, U., and Thomas, H. Preclinical profile of PKI166: a novel and potent EGF-R tyrosine kinase inhibitor for clinical development. Clin. Cancer Res., *5:* 3750s, 1999.

18. Bruns, C. J., Solorzano, C. C., Harbison, M. T., Ozawa, S., Tsan, R., Fan, D., Abbruzzese, J., Traxler, P., Buchdunger, E., Radinsky, R., and Fidler, I. J. Blockade of the epidermal growth factor receptor signaling by a novel tyrosine kinase inhibitor leads to apoptosis of endothelial cells and therapy of human pancreatic carcinoma. Cancer Res., *60:* 2926–2935, 2000.

19. Solorzano, C. C., Baker, C. H., Tsan, R., Traxler, P., Cohen, P., Buchdunger, E., Killion, J. J., and Fidler, I. J. Optimization for the blockade of the epidermal growth factor receptor signaling for therapy of human pancreatic carcinoma. Clin. Cancer Res., *7:* 2563–2572, 2001.

20. Uhlman, D. L., Nguyen, P., Manivel, J. C., Zhang, G., Hagen, K., Fraley, E., Aeppli, D., and Niehans, G. A. Epidermal growth factor receptor and transforming growth factor α expression in papillary and nonpapillary renal cell carcinoma: correlation with metastatic behavior and prognosis. Clin. Cancer Res., *8:* 913–920, 1995.

21. Atlas, I., Mendelsohn, J., Baselga, J., Fair, W. R., Masui, H., and Kumar, R. Growth regulation of human renal carcinoma cells: role of transforming growth factor α. Cancer Res., *52:* 3335–3339, 1992.

22. Moch, H., Sauter, G., Buchholz, N., Gasser, T. C., Bubendorf, L., Waldman, F. M., and Mihatsch, M. J. Epidermal growth factor receptor expression is associated with rapid tumor cell proliferation in renal cell carcinoma. Hum. Pathol., *11:* 1255–1259, 1997.

23. Hofmockel, G., Riess, S., Bassukas, I. D., and Dammrich, J. Epidermal growth factor family and renal cell carcinoma: expression and prognostic impact. Eur. Urol., *4:* 478–484, 1997.

24. Yoshida, K., Tosaka, A., Takeuchi, S., and Kobayashi, N. Epidermal growth factor receptor content in human renal cell carcinomas. Cancer (Phila.), *73:* 1913–1918, 1994.

25. Pettaway, C. A., Pathak, S., Greene, G., Ramirez, E., Wilson, M. R., Killion, J. J., and Fidler, I. J. Selection of highly metastatic variants of different human prostate carcinomas utilizing orthotopic implantation in nude mice. Clin. Cancer Res., *2:* 1627–1636, 1996.

26. Mori, S., Sawai, T., Teshima, T., and Kyogoku, M. A new decalcifying technique for immunohistochemical studies of calcified tissue, especially applicable to cell surface marker demonstration. J. Histochem. Cytochem., *36:* 111–114, 1988.

27. Baker, C. H., Solorazno, C. C., and Fidler, I. J. Blockade of vascular endothelial growth factor receptor signaling for therapy of metastatic human pancreatic cancer. Cancer Res., *62:* 1996–2003, 2002.

28. Petrylak, D. P., MacArthur, R. B., O'Connor, J., Shelton, G., Judge, T., Balog, J., Pfaff, C., Bagiella, E., Heitjan, D., Fine, R., Zuech, N., Sawczuk, I., Benson, M., and Olsson, C. A. Phase I trial of docetaxel with estramustine in androgen-independent prostate cancer. J. Clin. Oncol., *17:* 958–967, 1999.

29. Smith, D. C., Esper, P., Strawderman, M., Redman, B., and Poenta, K. J. Phase II trial of oral estramustine, oral etoposide, and intravenous paclitaxel in hormone-refractory prostate cancer. J. Clin. Oncol., *17:* 1664–1671, 1999.

30. Salomon, D., Brandt, R., Ciardiello, F., and Normanno, N. Epidermal growth factor-related peptides and their receptors in human malignancies. Crit. Rev. Oncol. Hematol., *19:* 183–232, 1995.

31. Mendelsohn, J., and Baselga, J. The EGF receptor family as targets for cancer therapy. Oncogene, *19:* 6550–6565, 2000.

32. Levitzki, A., and Gazit, A. Tyrosine kinase inhibition: an approach to drug development. Science (Wash. DC), *267:* 1782–1785, 1995.

33. Korc, M., Chandrasekar, B., Yamanaka, Y., Friess, H., Buchier, M., and Beger, H. G. Overexpression of the epidermal growth factor receptor in human pancreatic cancer is associated with concomitant increases in the levels of epidermal growth factor and transforming growth factor-α. J. Clin. Investig., *90:* 1352–1360, 1993.

34. Ullrich, A., Coussens, L., Hayflick, J. S., Dull, T. J., Gray, A., Tam, A. W., Lee, J., Yarden, Y., Libermann, T. A., and Schlessinger, J. Human epidermal growth factor receptor cDNA sequence and aberrant expression of the amplified gene in A431 epidermoid carcinoma cells. Nature (Lond.), *309:* 418–425, 1984.

35. Yamanaka, Y., Friess, H., Kobrin, M. S., Buchler, M., Beger, H. G., and Korc, M. Coexpression of epidermal growth factor receptor and ligands in human pancreatic cancer is associated with enhanced tumor aggressiveness. Anticancer Res., *13:* 565–569, 1993.

36. Perrotte, P., Matsumoto, T., Inoue, K., Kuniyasu, H., Eve, B. Y., Hicklin, D. J., Radinsky, R., and Dinney, C. P. N. Antiepidermal growth factor receptor antibody C225 inhibits angiogenesis in human transitional cell carcinoma growing orthotopically in nude mice. Clin. Cancer Res., *5:* 257–265, 1999.

37. Ciardiello, F., Damiano, V., Bianco, R., Bianco, C., Fontanini, C., De Laurentiis, M., De Placido, S., Mendelsohn, J., Bianco, A. R., and Tortora, G. Antitumor activity of combined blockade of epidermal growth factor receptor and protein kinase A. J. Natl. Cancer Inst. (Bethesda), *88:* 1770–1776, 1996.

38. Huang, S. M., Bock, J. M., and Harari, P. M. Epidermal growth factor receptor blockade with C225 modulates proliferation, apoptosis, and radiosensitivity in squamous cell carcinomas if the head and neck. Cancer Res., *59:* 1935–1940, 1999.

39. Baselga, J., Norton, L., Masui, H., Pandiella, A., Coplan, K., Miller, W. H. J., and Mendelsohn, J. Antitumor effects of doxorubicin in combination with antiepidermal growth factor receptor monoclonal antibodies. J. Natl. Cancer Inst. (Bethesda), *85:* 1327–1333, 1993.

40. Karashima, T., Sweeney, P., Slaton, J. W., Kim, S. J., Kedar, D., Izawa, J. I., Fan, Z., Pettaway, C., Hicklin, D. J., Shuin, T., and Dinney, C. P. N. Inhibition of angiogenesis by the antiepidermal growth factor receptor antibody ImClone C225 in androgen-independent prostate cancer growing orthotopically in nude mice. Clin. Cancer Res., *8:* 1253–1264, 2002.

41. van Gog, F. B., Brakenhoff, R. H., and Stigter-van Snow, G. B. Perspectives of combined radioimmunotherapy and anti-EGF-R antibody therapy for the treatment of residual head and neck cancer. Int. J. Cancer, *77:* 13–18, 1998.

42. Aboud-Pirak, E., Hurwitz, E., Pirak, M. E., Bellot, F., Schlessinger, J., and Sela, M. Efficacy of antibodies to epidermal growth factor receptor against KB carcinoma *in vitro* and in nude mice. J. Natl. Cancer Inst. (Bethesda), *80:* 1605–1611, 1988.

43. Massagué, J. TGF-β signal transduction. Annu. Rev. Biochem., *67:* 753–771, 1998.

44. Boerner, P., Resnick, R. J., and Racker, E. Stimulation of glycolysis and amino acid uptake in NRK-49F cells by transforming growth factor-β and epidermal growth factor. Proc. Natl. Acad. Sci. USA, *82:* 1350–1353, 1985.

45. Inman, W. H., and Colowick, S. P. Stimulation of glucose uptake by transforming growth factor-β: evidence for the requirement of epidermal growth factor-receptor activation. Proc. Natl. Acad. Sci. USA, *82:* 1346–1349, 1985.

46. Tatsuyama, K., Maezawa, Y., Baba, H., Imamura, Y., and Fukuda, M. Expression of various growth factors for cell proliferation and cytodifferentiation during fracture repair of bone. Eur. J. Histochem., *44:* 269–278, 2000.

47. Baker, C. H., Kedar, D., McCarty, M. F., Tsan, R., Weber, K. L., Bucana, C. D., and Fidler, I. J. Blockade of epidermal growth factor receptor signaling on tumor cells and tumor-associated endothelial cells for therapy of human carcinomas. Am. J. Pathol., *161:* 929–938, 2002.

48. Syridopoulos, I., Brogi, E., Kearney, M., Sullivan, A. B., Cetrulo, C., Isner, M., and Losordo, D. W. Vascular endothelial growth factor inhibits endothelial cell apoptosis induced by tumor necrosis factor-α: balance between growth and death signals. J. Mol. Cell. Cardiol., *29:* 1321–1330, 1997.

49. Gerber, H. P., Dixit, V., and Ferrera, N. Vascular endothelial growth factor induces expression of the antiapoptotic proteins Bcl-2 and A1 in vascular endothelial cells. J. Biol. Chem., *273:* 13313–13316, 1998.

50. Nor, J. E., Christensen, J., Mooney, D. J., and Polverini, P. J. Vascular endothelial growth factor (VEGF)-mediated angiogenesis is associated with enhanced endothelial cell survival and induction of Bcl-2 expression. Am. J. Pathol., *154:* 375–384, 1999.

51. Watanabe, Y., and Dvorak, H. V. Vascular permeability factor/vascular endothelial growth factor inhibits anchorage-disruption-induced apoptosis in microvessel endothelial cells by inducing scaffold formation. Exp. Cell Res., *233:* 340–349, 1997.

52. Uckun, F. M., Narla, R. K., Jun, X., Zeren, T., Venkatachalam, T., Waddick, K. G., Rostostev, A., and Myers, D. E. Cytotoxic activity of epidermal growth factor genistein against breast cancer cells. Clin. Cancer Res., *4:* 901–912, 1998.

53. Uckun, F. M., Narla, R. K., Zeren, T., Yanishevski, Y., Myers, D. E., Waurzyniak, B., Ek, O., Schneider, E., Messinger, Y., Chelstrom, L. M., Gunther, R., and Evans, W. *In vivo* toxicity, pharmacokinetics, and anticancer activity for genistein linked to recombinant human epidermal growth factor. Clin. Cancer Res., *4:* 1125–1134, 1998.

54. Mendelsohn, J. Epidermal growth factor receptor inhibition by a monoclonal antibody as anticancer therapy. Clin. Cancer Res., *3:* 2703–2707, 1997.

55. Hirata, A., Ogawa, S., Kometani, T., Kuwano, T., Naito, S., Kuwano, M., and Ono, M. ZD 1839 (Iressa) induces antiangiogenic effects through inhibition of epidermal growth factor receptor tyrosine kinase. Cancer Res., *62:* 2554–2560, 2002.

56. Fidler, I. J., Yano, S., Zhang, R-D., Fujimaki, T., and Bucana, C. D. The seed and soil hypothesis: vascularization and brain metastasis. Lancet Oncol., *3:* 53–57, 2002.

Clinical Cancer Research

Blockade of Epidermal Growth Factor Receptor Signaling in Tumor Cells and Tumor-associated Endothelial Cells for Therapy of Androgen-independent Human Prostate Cancer Growing in the Bone of Nude Mice

Sun-Jin Kim, Hisanori Uehara, Takashi Karashima, et al.

Clin Cancer Res 2003;9:1200-1210.